Supplementary data

Rhodamine-based highly specific fluorescent probe for the *in situ* and in *vivo* imaging of the biological signalling molecule salicylic acid

Pei-Yi Wang, [†] [a] Xue Luo, [†] [a] Lin-Lin Yang, [a] Yuan-Chao Zhao, [a] Rong Dong, [a] Zhong Li [b] and Song Yang*[a,b]

Contents

1. Materials and methods

All chemicals were purchased from commercial suppliers and used without further purification. All the solvents were of analytic grade. Deionized distilled water was used throughout. All reactions were magnetically stirred and monitored by thin-layer chromatography (TLC) using Spectrochem GF254 silica gel coated plates. ^{1}H and ^{13}C NMR spectra were measured on a JEOL-ECX 500 NMR spectrometer at room temperature using TMS as an internal standard. Mass spectra were recorded on an Agilent LC/MSD Trap VL mass spectrometer. Fluorescence spectra measurements were performed on a Fluoromax-4 spectrofluorimeter (Horiba Trading CO., LTD). UV–vis spectra were performed on a TU-1900 spectrophotometer (Beijing Pgeneral Instrument Co., China). Fluorescence imaging was performed using an OLYMPUS FVMPE-RS inverted fluorescence microscope with a 25×objective lens. The following abbreviations are used to describe spin multiplicities in ^{1}H NMR spectra: s = singlet, d = doublet, t = triplet, m = multiplet, q = quartet.

The stock solutions of probe **1** and **2** (1.0×10^{-3} M) were prepared in methanol and acetonitrile, respectively. Analyte stock solutions (1.0×10^{-2} M) of salicylic acid (SA) Phenol, salicylaldehyde, methyl salicylate (MeSA), Pyrocatechol (Catechol), acetylsalicylic acid (ASA), benzoic acid (BA), anthranilic acid (2-NH_2BA), 2-methylbenzoic acid (2-MeBA), 2-methoxybenzoic acid (2-MeOBA), 3-hydroxybenzoic acid (3-OHBA) and 4-hydroxybenzoic acid (4-OHBA) were prepared in methanol and acetonitrile, respectively. The procedures to prepare samples for fluorescence and UV-vis spectra measurement were as follows: 100 μL of 1 mM stock solution of probe was added into a volumetric flask (10 mL), then appropriate amount of analytes was added into the volumetric flask and the mixture was diluted to 10 mL with corresponding solvent. Spectral data were usually recorded at 10 min after the addition of corresponding solvent.

2. Synthesis of probe 1 and probe 2

(1) **Synthesis of probe 1** [1]

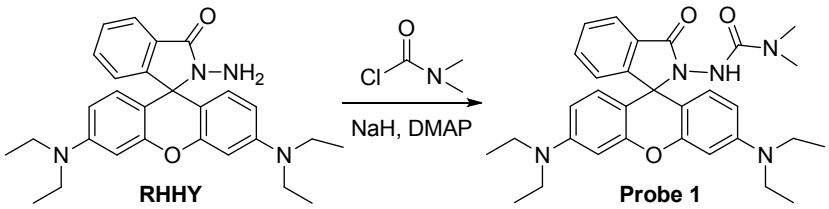

A mixture of Rhodamine B hydrazide (**RHHY**) (1.83 g, 4 mmol), NaH (0.48 g, 20 mmol), 4-dimethylaminopyridine (DMAP, 0.24 g, 2 mmol) and 30 mL dry acetonitrile was stirred in a three-necked flask. Then dimethylcarbamyl chloride (2.4 mL, 20 mmol) was added to the solution and the mixture was refluxed overnight. The color of the solution changed from gray to red gradually. After that, the solid of the mixture was filtered off and the organic solution was washed by water, dried with anhydrous sodium sulfate, filtered, and followed by the removal of the solvent under vacuum. Finally, the product was purified by column chromatography on silica gel and eluted with petrol ether-ethyl acetate (3 : 1 to 1 : 2) to give tawny solid. The nearly pure product was recrystallized in ethyl acetate to give colorless crystals suitable for X-ray crystallography in 41.3% yield (0.87 g). ^{1}H NMR (500 MHz, $CDCl_3$) δ 7.95 (d, J = 7.2 Hz, 1H), 7.53–7.43 (m, 2H), 7.12 (d, J = 7.3 Hz, 1H), 6.61 (d, J = 8.8 Hz, 2H), 6.39 (d, J = 2.5 Hz, 2H), 6.30 (dd, J = 8.9, 2.5 Hz, 2H), 5.76 (s, 1H), 3.33 (qd, J = 7.2, 2.3 Hz, 8H, NCH_2), 2.72 (s, 6H, NCH_3), 1.16 (t, J = 7.0 Hz, 12H, $NCH_2\underline{CH_3}$); ^{13}C NMR (125 MHz, $CDCl_3$) δ 166.5, 156.7, 153.9, 151.6, 148.9, 133.2, 129.5, 129.2, 128.3, 124.2, 123.5, 108.0, 104.8, 97.7, 66.4, 44.4, 36.6, 12.7. Anal. Calcd for $C_{31}H_{37}N_5O_3$: C, 70.56; H, 7.07; N, 13.27. Found: C, 70.53; H, 7.05; N, 13.29. ESI$^+$-MS, m/z = 550.3, $[M + Na]^+$, calc. for $C_{31}H_{37}N_5O_3$ = 527.29.

(2) **Synthesis of probe 2**

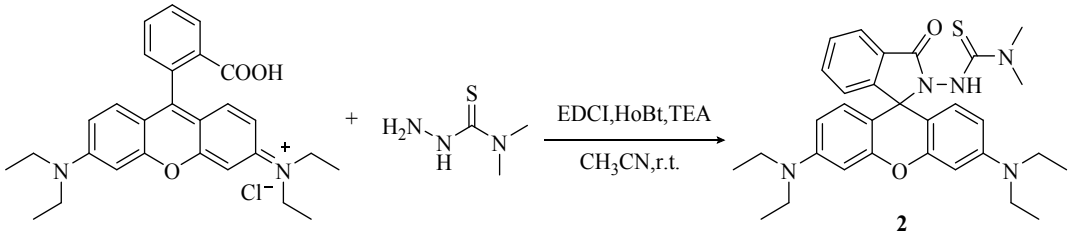

A mixture of Rhodamine B (0.223 g, 0.48 mmol), HoBt (0.0648 g, 0.48 mmol), EDCI (0.0938 g, 0.48 mmol) and 5 mL acetonitrile was stirred in a 25 mL three-necked flask for 4 h. Then 4, 4-dimethyl-3-thiosemicarbazide (0.0486 g, 0.40 mmol) and triethylamine (TEA, 112 μL) were added to the mixture along with the changes in the solution color from red to purple

gradually. The mixture was reacted for 12 h at room temperature, and monitored by thin layer chromatographic (TLC). After that, the solvent was removed under reduced pressure and extracted with dichloromethane. Finally, the product was purified by TLC on silica gel with dichloromethane-methanol (4:1) and crystallized in ethyl acetate to afford 0.0255 g of compound **2** in 10.4% yield. ^{1}H NMR (500 MHz, $CDCl_3$) δ 7.98 (d, *J* = 7.4 Hz, 1H), 7.56 (dtd, *J* = 25.8, 7.4, 1.0 Hz, 2H), 7.20 (d, *J* = 7.6 Hz, 1H), 6.45 (d, *J* = 2.4 Hz, 4H), 6.27 (dd, *J* = 8.9, 2.6 Hz, 2H), 6.23 (s, 1H), 3.34 (qd, *J* = 7.2, 2.3 Hz, 8H, NCH_2), 2.89 (s, 6H, NCH_3), 1.16 (t, *J* = 7.0 Hz, 12H, $NCH_2\underline{CH_3}$); ^{13}C NMR (125 MHz, $CDCl_3$) δ 187.6, 166.1, 154.2, 150.3, 149.2, 133.7, 129.6, 128.6, 128.2, 124.5, 123.5, 107.7, 104.0, 98.1, 67.6, 44.4, 42.2, 12.6. ESI^+-MS, m/z = 544.3, $[M+H]^+$, calc. for $C_{31}H_{37}N_5O_2S$ = 543.27.

3.Determination of fluorescence quantum yields

Probe **2** exhibited fluorescence quantum yield of Φ_{FL} = 0.07 (relative to the standard rhodamine B in methanol, Φ_{std} = 0.65),[2] calculated as follows:

$$\Phi_{unk} = \Phi_{std}\left(\frac{F_{unk}}{F_{std}}\right)\left(\frac{A_{std}}{A_{unk}}\right)\left(\frac{\eta_{unk}}{\eta_{std}}\right)^2$$

Where Φ_{unk} is the fluorescence quantum yield of the probe **2**, Φ_{std} is the quantum yield of the standard, F_{unk} and F_{std} are the integrated fluorescence intensity of the probe **2** and the standard, respectively, A_{unk} and A_{std} are the absorbance's of probe **2** and the standard at the absorption wavelength, respectively, η_{unk} and η_{std} are the refractive indices of corresponding solutions.

4.Calculation of detection limit

The detection limits of probe **1** and **2** for SA were calculated by signal-to-noise ratio (S/N).[3] The fluorescence intensity of probes without target analytes were measured 20 times at designated wavelengths. On the basis of these data, the average fluorescence intensity ($average_{blank}$) along with the associated standard deviation (SD_{blank}) was determined, and the SD_{blank} was considered as the noise (N) of our detection system. Subsequently, the fluorescence intensity of probe by adding corresponding analyte with a relatively low concentration were measured for five times, and the

average value ($average_{sample}$) was recorded. Finally, S/N was calculated as follows:

$$S/N = \left(\left|average_{sample} - average_{blank}\right|\right)/SD_{blank}$$

If the S/N value fell within the range of 3 to 5, suggesting that the corresponding concentration was determined as the detection limit.

5.Cell culture

The NRK-52E cells were grown in Dulbecco's modified Eagle's medium (DMEM) supplemented with 10% fetal bovine serum (FBS) and 1% penicillin–streptomycin. The cells were plated in a 12-well plate containing the treated cover glass at a density of 1.5×10^4 cells per well in culture media, incubated under an humidified atmosphere of 5% CO_2 and 95% air at 37 °C for 24 h.

6. Crystal structure of probe 1

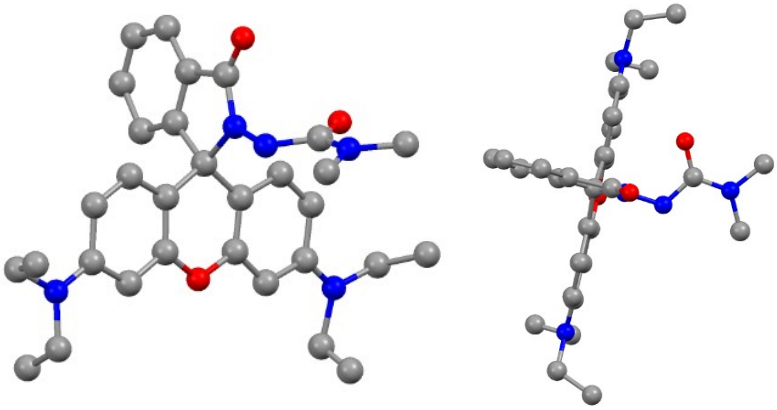

Fig. S1 Crystal structure of probe **1** and all the hydrogen atoms are omitted for clarity (CCDC 1472928; grey atom, C; red atom, O; blue atom, N).

7. The ^{1}H NMR, ^{13}C NMR and mass spectra of probe 2

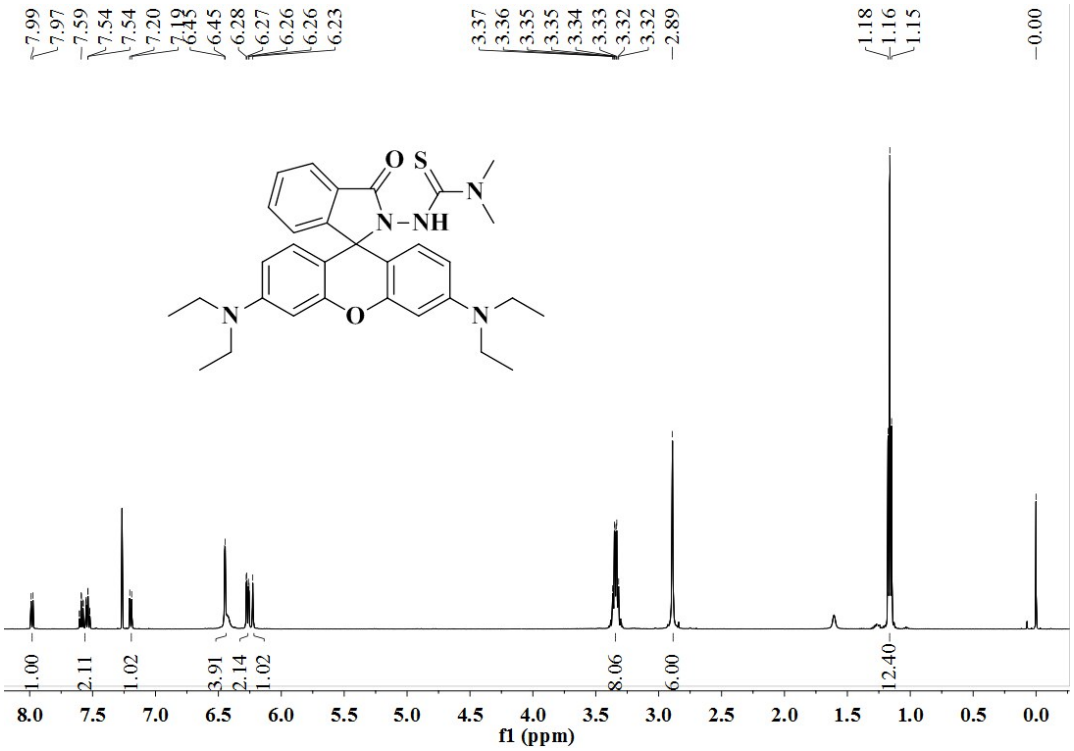

Fig. S2 ^{1}H NMR of compound **2** in $CDCl_3$ (500 MHz).

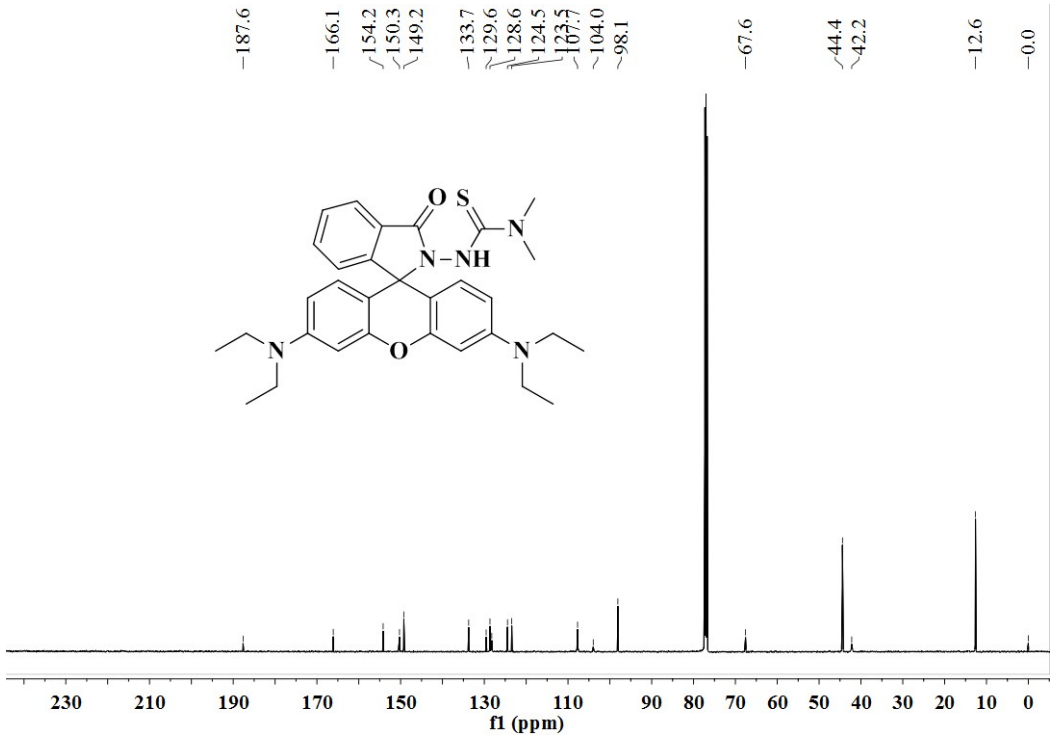

Fig. S3 ^{13}C NMR of compound **2** in $CDCl_3$ (125 MHz).

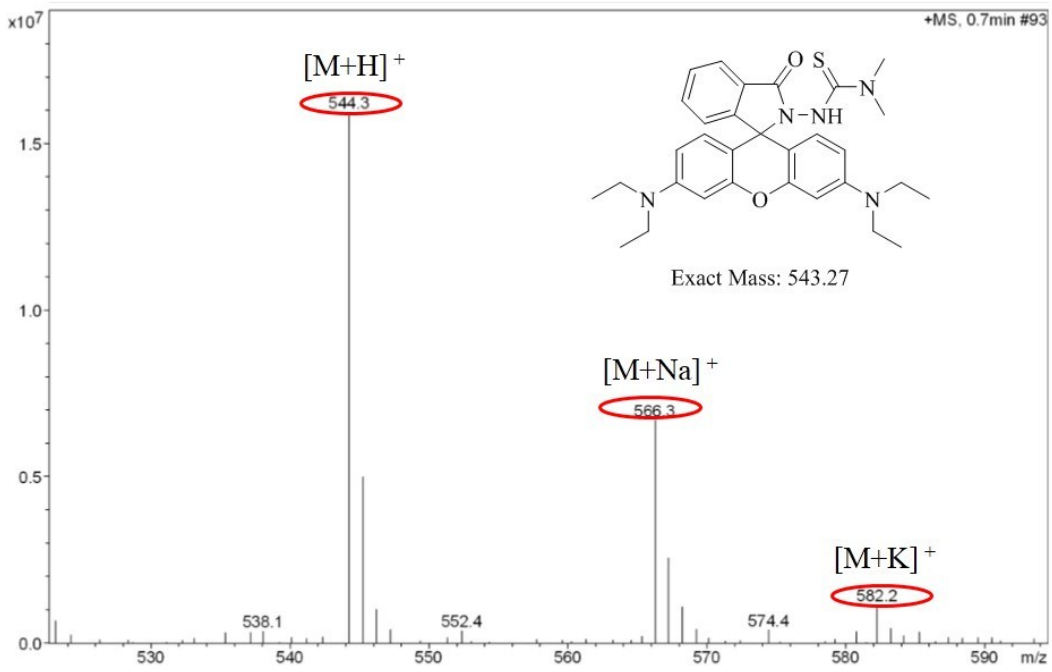

Fig. S4 ESI-Mass spectrum of compound **2**.

8. The sensitivity of probe 1 for SA in different solvent

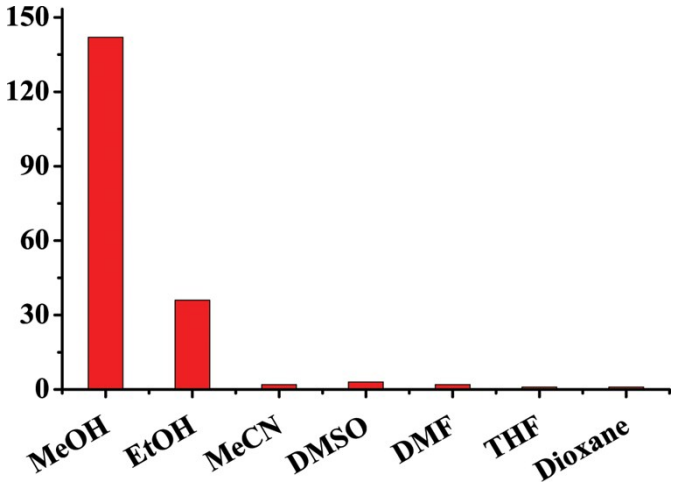

Fig. S5 The enhancement fold of emission intensity at 577 nm of **1** (10 μM) upon addition of SA (100 μM) in different solvent (λ_{ex} = 550 nm, slits: 2 nm/2 nm).

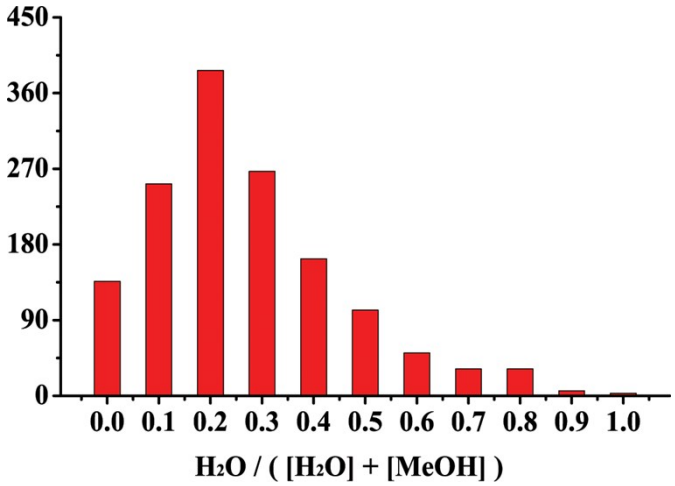

Fig. S6 The enhancement fold of emission intensity at 577 nm of **1** (10 μM) upon addition of SA (100 μM) in the mixed CH_3OH-H_2O solvent (λ_{ex} = 550 nm, slits: 2 nm/2 nm).

9. Competition experiments of probe 1 for SA analogues

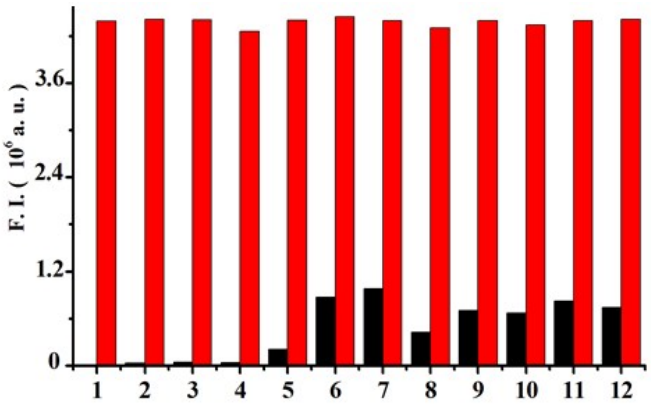

Fig. S7 Competition experiments for adding 550 μM SA into the premixed solution consisting of probe **1** (10 μM) with various SA analogs (550 μM) (1) blank, (2) MeSA, (3) Phenol, (4) Catechol, (5) salicylaldehyde, (6) ASA, (7) BA, (8) 2-aminoBA, (9) 3-OHBA, (10) 4-OHBA, (11) 2-MeBA, (12) 2-MeOBA, black bars: fluorescence intensity at 577 nm for probe **1** with SA analogs, red bars: after adding SA into the premixed probe **1** with SA analogs. Experimental conditions: (λ_{ex} = 550 nm, slits: 2 nm/2 nm, CH_3OH:H_2O = 4:1, V/V).

10. The fluorescence and UV-Vis titration curve of probe 1 with SA

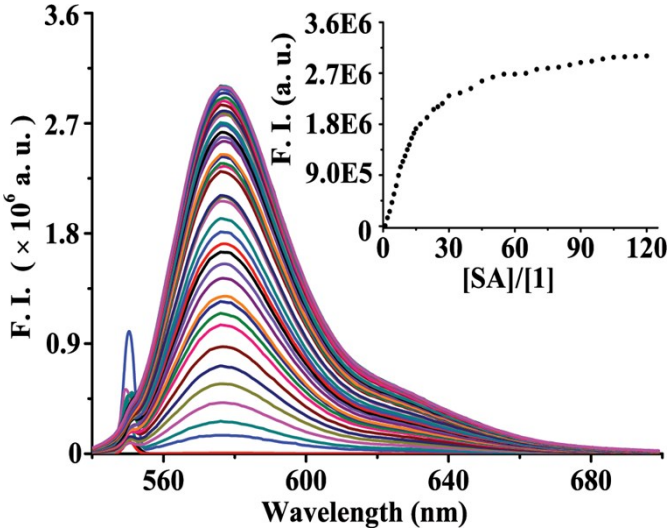

Fig. S8 Fluorescence emission spectra obtained during the titration of probe **1** (10 μM) with SA (from 0 to 1200 μM) in the mixed solution (CH_3OH:H_2O = 4:1, V/V). The inset shows changes of the fluorescence intensity at 577 nm (λ_{ex} = 550 nm, slits: 2 nm/2 nm).

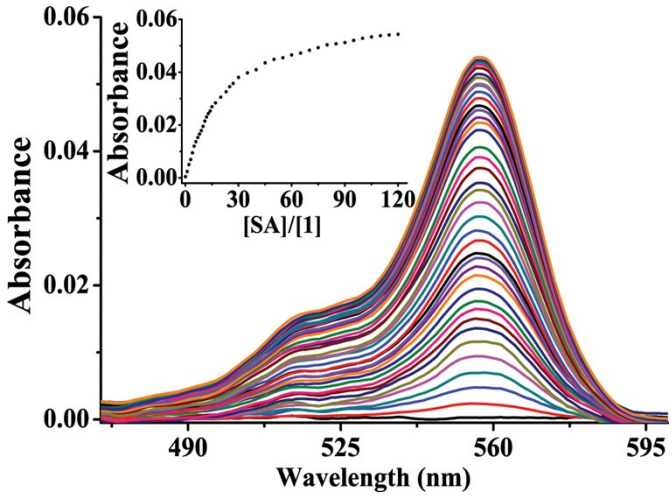

Fig. S9 Absorption spectra obtained during the titration of probe **1** (10 μM) with SA (from 0 to 1200 μM) in the mixed solution (CH_3OH:H_2O = 4:1, V/V). The inset shows changes of the absorbance at 555 nm.

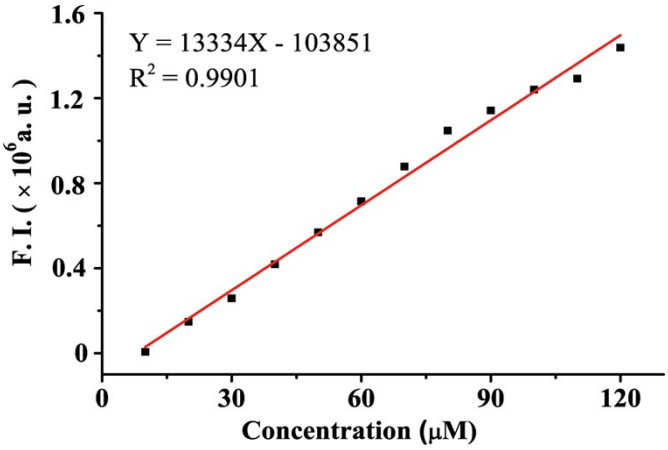

Fig. S10 The linear fluorescence (at 577 nm) change of probe **1** (10 μM) with SA (10-120 μM).

11. Job's plot and Benesi-Hildebrand plot of probe 1 with SA

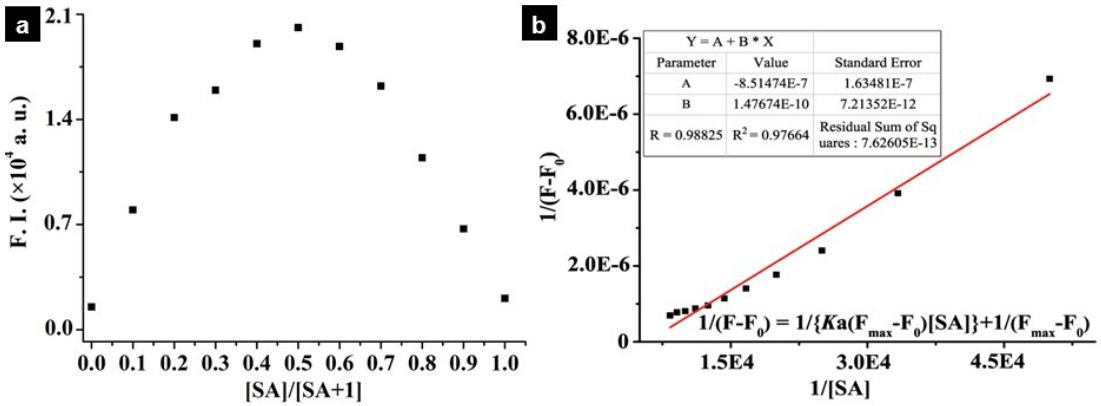

Fig. S11 Job's plot (a) and Benesi-Hildebrand plot (b) of probe **1** with SA. Binding constant ($K_a = 5.77 \times 10^3$ μM^{-1}) was determined by fluorescence method (λ_{ex} = 550 nm, slits: 2 nm/2 nm).

12. The sensitivity of probe 2 for SA in different solvent

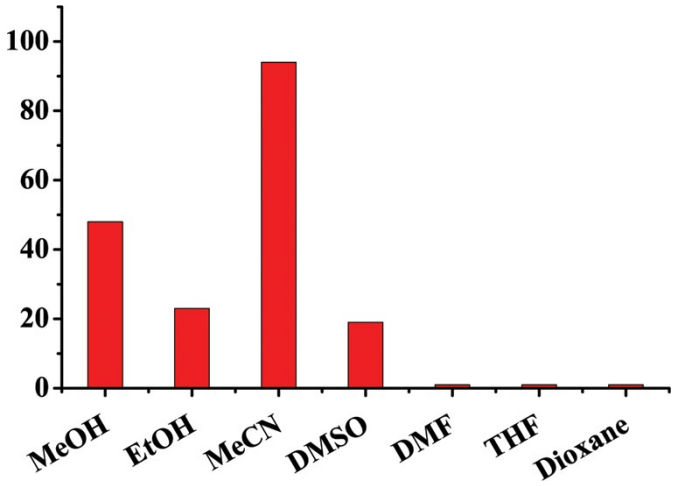

Fig. S12 The enhancement fold of emission intensity at 583 nm of **2** (10 μM) upon addition of SA (100 μM) in different solvent (λ_{ex} = 553 nm, slits: 2 nm/2 nm).

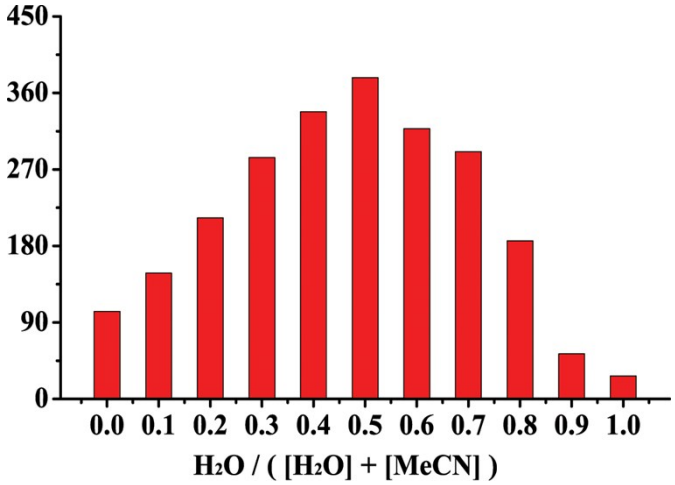

Fig. S13 The enhancement fold of emission intensity at 583 nm of **2** (10 μM) upon addition of SA (100 μM) in the mixed CH_3CN-H_2O solvent (λ_{ex} = 553 nm, slits: 2 nm/2 nm).

13. Competition experiments of probe 2 for SA analogues

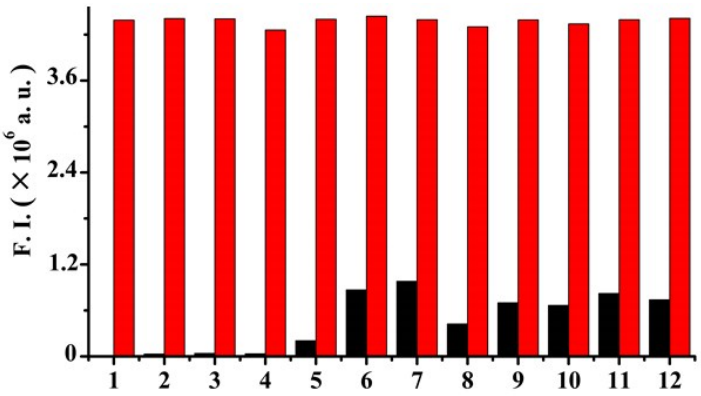

Fig. S14 Competition experiments for adding 200 μM SA into the premixed solution consisting of probe **2** (10 μM) with various SA analogs (200 μM) (1) blank, (2) MeSA, (3) Phenol, (4) Catechol, (5) salicylaldehyde, (6) ASA, (7) BA, (8) 2-aminoBA, (9) 3-OHBA, (10) 4-OHBA, (11) 2-MeBA, (12) 2-MeOBA, black bars: fluorescence intensity at 577 nm for probe **2** with SA analogs, red bars: after adding SA into the premixed probe **2** with SA analogs. Experimental conditions: (λ_{ex} = 553 nm, slits: 2 nm/2 nm, CH_3CN:H_2O = 1:1, V/V).

14. The fluorescence and UV-Vis titration curve of probe 2 with SA

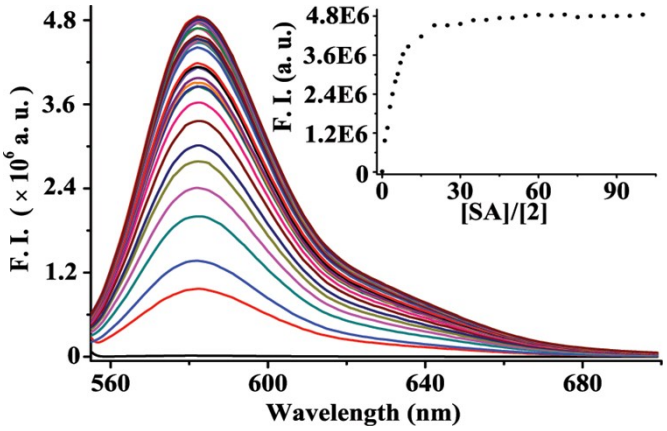

Fig. S15 Fluorescence emission spectra obtained during the titration of probe **2** (10 μM) with SA (from 0 to 1000 μM) in the mixed solution (CH_3CN:H_2O = 1:1, V/V). The inset shows changes of the fluorescence intensity at 583 nm (λ_{ex} = 553 nm, slits: 2 nm/2 nm).

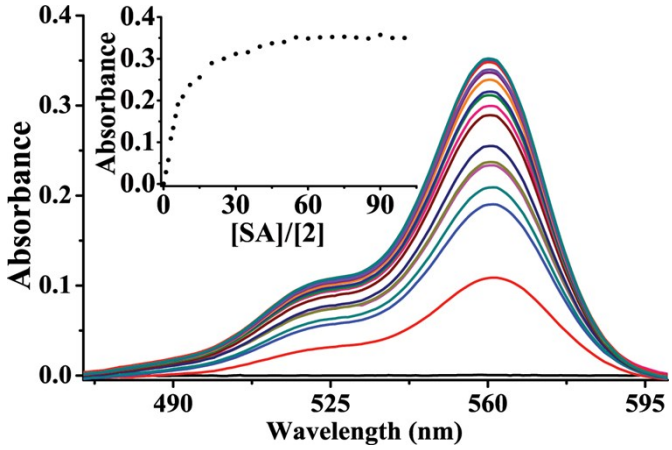

Fig. S16 Absorption spectra obtained during the titration of probe **2** (10 μM) with SA (from 0 to 1000 μM) in the mixed solution (CH_3CN:H_2O = 1:1, V/V). The inset shows changes of the absorbance at 559 nm.

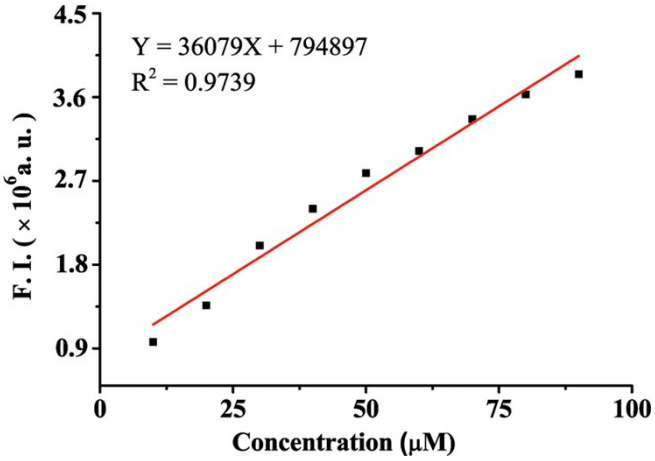

Fig. S17 The linear fluorescence (at 583 nm) change of probe **2** (10 μM) with SA (10-90 μM).

15. Job's plot and Benesi-Hildebrand plot of probe 2 with SA

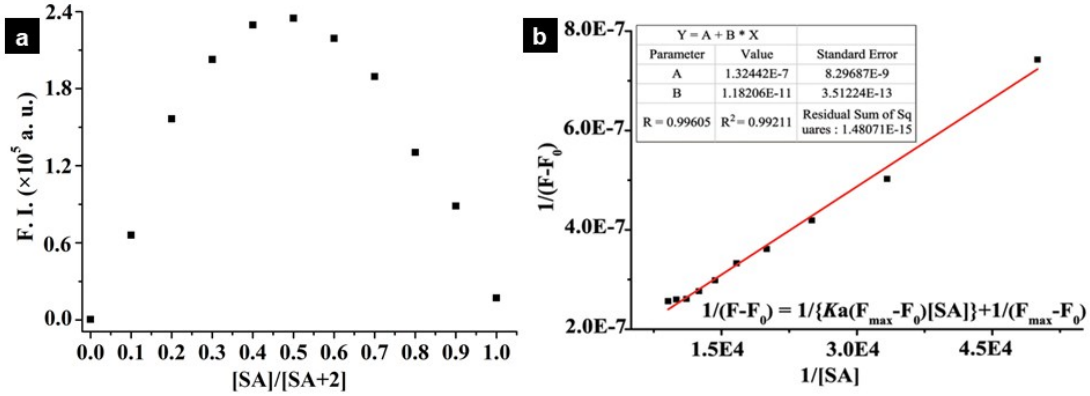

Fig. S18 Job's plot (a) and Benesi-Hildebrand plot (b) of probe **2** with SA. Binding constant (K_a = 1.12 × 10^4 μM^{-1}) was determined by fluorescence method (λ_{ex} = 553 nm, slits: 2 nm/2 nm).

16. Chemical shift of SA and probe 1 or 2 after formation of the complex

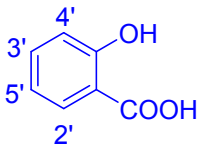

Table S1 Chemical shift of SA after formation of the complex probe **1**-SA with different molar ratios.

Chemical shift (ppm)	proton			
	2’	3’	4’	5’
SA	7.94	7.54	7.02	6.94
SA : probe **1**=0.5 : 1	7.86	7.42	6.91	6.84
SA : probe **1**=1 : 1	7.88	7.44	6.94	6.87
SA : probe **1**=2 : 1	7.89	7.46	6.96	6.89
Shift $_{\text{SA : probe 1=0.5 : 1}}$	-0.08	-0.12	-0.11	-0.10
Shift $_{\text{SA : probe 1=1 : 1}}$	-0.06	-0.10	-0.08	-0.07
Shift $_{\text{SA : probe 1=2 : 1}}$	-0.05	-0.08	-0.06	-0.05

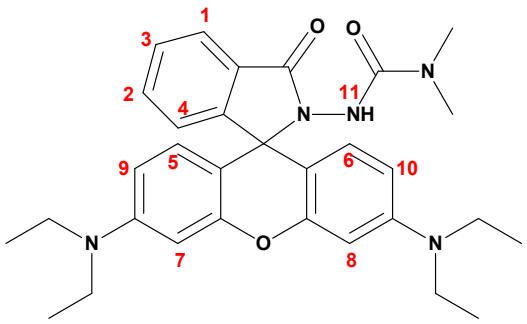

Table S2 Chemical shift of probe **1** after formation of the complex probe **1**-SA with different molar ratios.

Chemical shift (ppm)	proton						
	1	2、3	4	5、6	7、8	9、10	11
Probe **1**	7.95	7.47	7.12	6.60	6.38	6.30	5.75
SA : probe **1**=0.5 : 1	7.96	7.49	7.13	6.59	6.39	6.30	6.02
SA : probe **1**=1 : 1	7.98	7.52	7.16	6.57	6.39	6.30	6.52
SA : probe **1**=2 : 1	7.99	7.53	7.17	6.57	6.41	6.31	6.73
Shift $_{\text{SA : probe 1=0.5 : 1}}$	0.01	0.02	0.01	-0.01	0.01	0	0.27
Shift $_{\text{SA : probe 1=1 : 1}}$	0.02	0.05	0.04	-0.03	0.01	0	0.77
Shift $_{\text{SA : probe 1=2 : 1}}$	0.04	0.06	0.05	-0.03	0.03	0.01	0.98

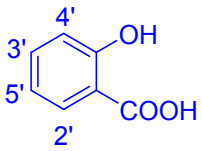

Table S3 Chemical shift of SA after formation of the complex probe **2**-SA with different molar ratios.

Chemical shift (ppm)	proton			
	2’	3’	4’	5’
SA	7.94	7.54	7.02	6.94
SA : probe **2**=0.5 : 1	7.89	7.42	6.97	6.89
SA : probe **2**=1 : 1	7.90	7.47	6.97	6.89
SA : probe **2**=2 : 1	7.91	7.48	6.97	6.90
Shift $_{\text{SA : probe 2=0.5 : 1}}$	-0.05	-0.12	-0.05	-0.05
Shift $_{\text{SA : probe 2=1 : 1}}$	-0.04	-0.07	-0.05	-0.05
Shift $_{\text{SA : probe 2=2 : 1}}$	-0.03	-0.06	-0.05	-0.04

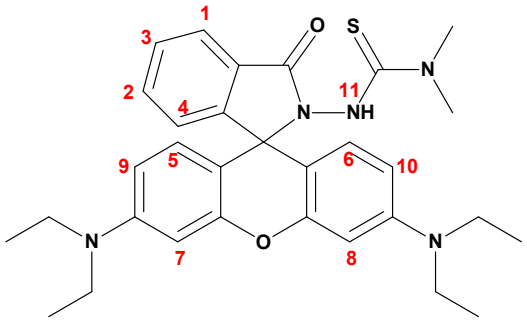

Table S4 Chemical shift of probe **2** after formation of the complex probe **2**-SA with different molar ratios.

Chemical shift (ppm)	proton						
	1	2	3	4	5-8	9、10	11
Probe **2**	7.97	7.58	7.53	7.19	6.44	6.26	6.23
SA : probe **2**=0.5 : 1	7.99	7.59	7.54	7.20	6.46	6.27	6.43
SA : probe **2**=1 : 1	8.00	7.59	7.54	7.20	6.47	6.28	6.52
SA : probe **2**=2 : 1	8.01	7.60	7.55	7.21	6.49	6.30	6.68
Shift $_{\text{SA : probe 2=0.5 : 1}}$	0.02	0.01	0.01	0.01	0.02	0.02	0.20
Shift $_{\text{SA : probe 2=1 : 1}}$	0.03	0.01	0.01	0.01	0.03	0.03	0.29
Shift $_{\text{SA : probe 2=2 : 1}}$	0.04	0.02	0.02	0.02	0.05	0.04	0.45

17. MALDI-TOF MS (Matrix assisted laser desorption lonization time of flight mass spectrometry) and HRMS for probe 2 (or probe 1) after treatment with SA, and ^{1}H NMR spectrum for the newly product containing 1,3,4-oxadiazole ring.

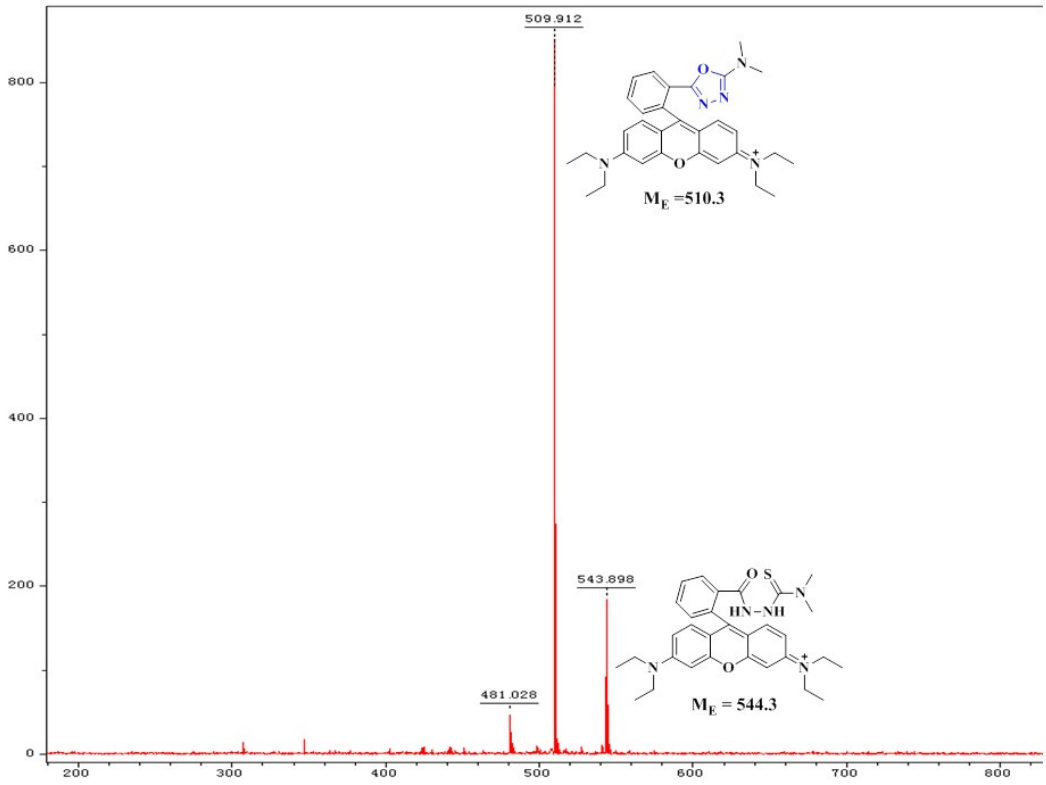

Fig. S19 MALDI-TOF MS for probe **2** with SA.

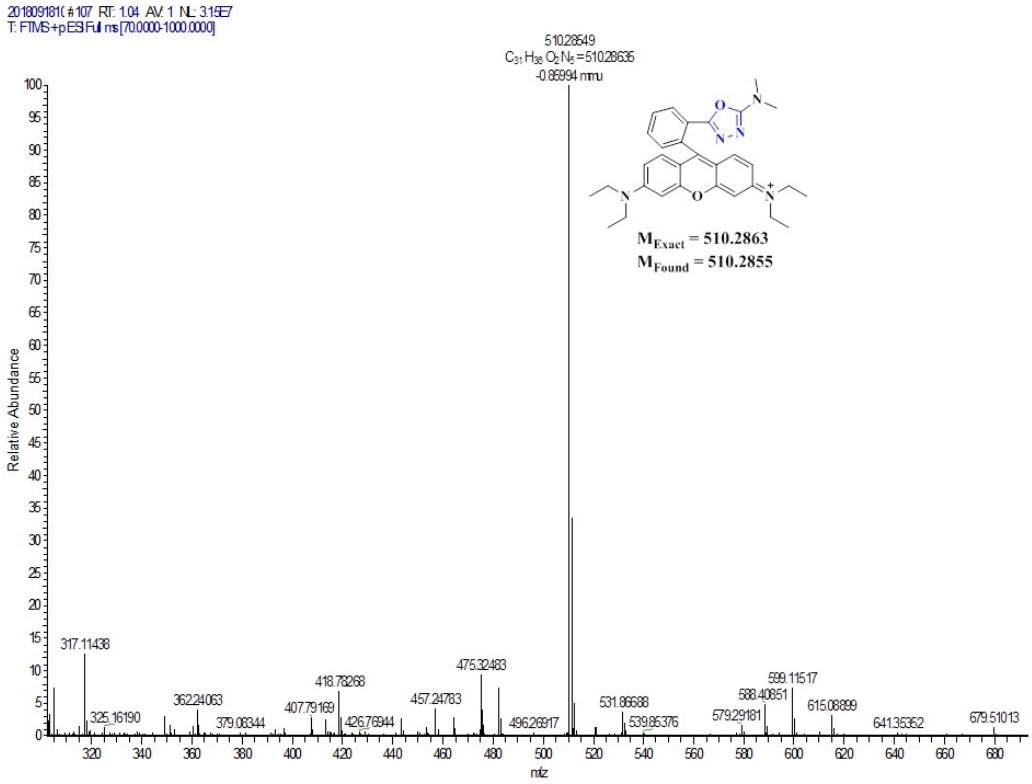

Fig. S20 HRMS for the new product containing 1,3,4-oxadiazole ring for probe **2** induced by SA.

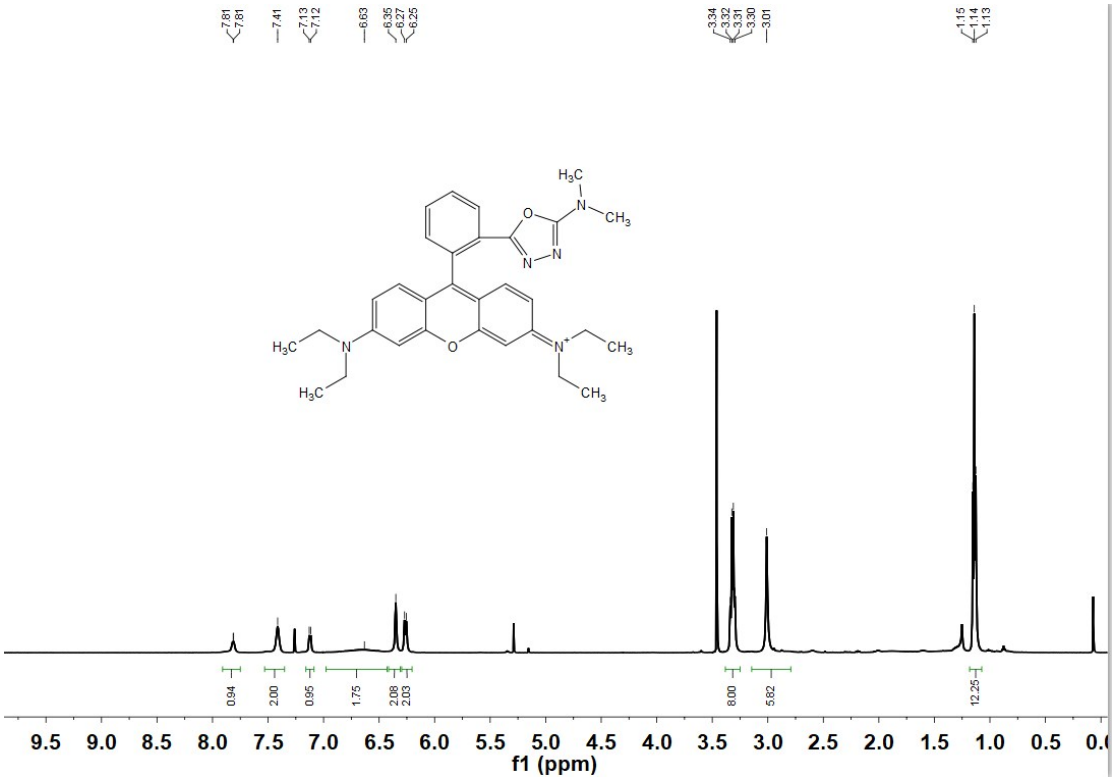

Fig. S21 ^{1}H NMR spectrum for the newly product containing 1,3,4-oxadiazole ring (500 MHz, $CDCl_3$).

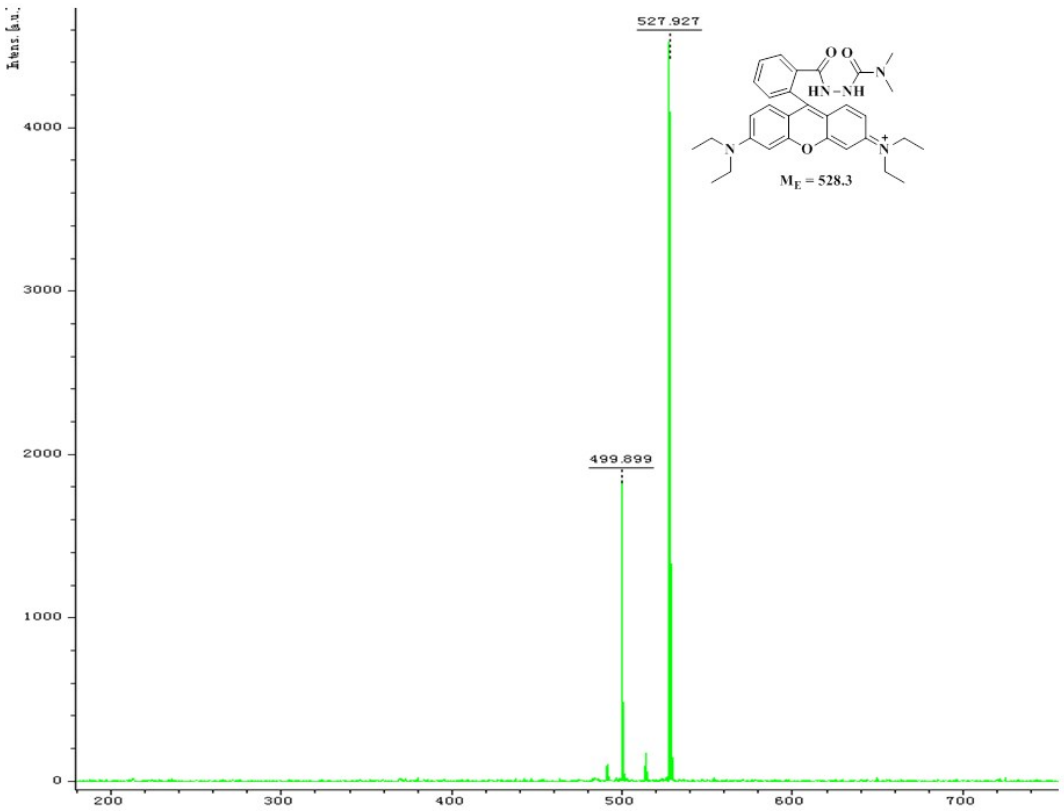

Fig. S22 MALDI-TOF MS for probe **1** with SA

18. Cell imaging of probe 1 with SA

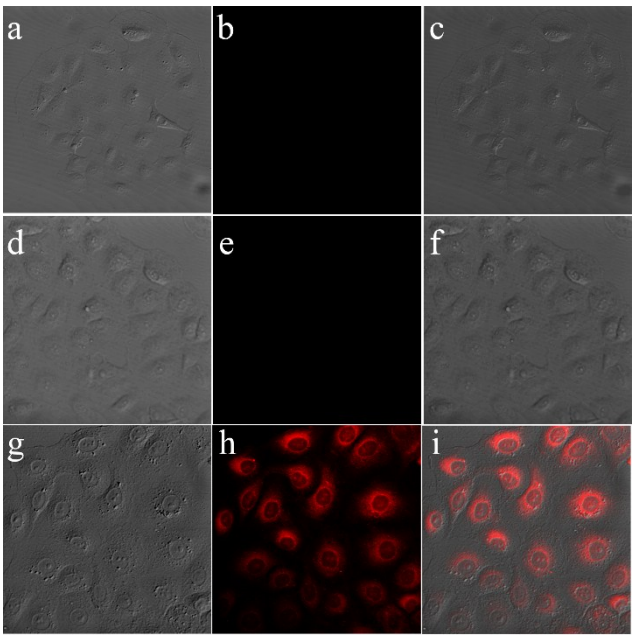

Fig. S23 Laser scanning two-photon fluorescence microscope images of NRK-52E cells: (a) bright-field and (b) fluorescence image of NRK-52E cells, (c) merged image of a and b; (d)

bright-field and (e) fluorescence image of NRK-52E cells incubated with 40 μM probe **1** for 30 min at 37 °C, (f) merged image of d and e; (g) bright-field and (h) fluorescence image of NRK-52E cells incubated with 40 μM probe **1** and then 400 μM SA for 2 h at 37 °C, (i) merged image of g and h. Red channel, λ_{ex} = 1125 nm.

19. Comparison of the LOD of the proposed method and other works

Table S5 Comparison of the LOD of the proposed method and other works

Methods	LOD	References
LC [4]	40 ng·mL^{-1}	4
LC-MS [5]	6.57 ng·mL^{-1}	5
HPLC [6]	20 ng·mL^{-1}	6a
	200 ng·mL^{-1}	6b
UHPLC−MS/MS [7]	8.9 ng·g^{-1}	7
Sequential injection chromatography [8]	1000 ng·mL^{-1}	8
Liquid Membrane Electrod [9]	60000 nM	9
Differential-pulse voltammetry [10]	0.5 ppm	10
Capillary zone electrophoresis [11]	420 ng·mL^{-1}	11
A coupled enzymatic assay [12]	6.5 nM	12
Biosensor [13]	3500 nM	13
Probe [14]	4.2 ng·mL^{-1}	14
CdTe quantum dots [15]	150 ng·mL^{-1}	15
Proposed work	2 nM	

References

1. Y. C. Zhao, C. Chen, B. Chen, P. Y. Wang, Z.-B. Wu, H. Li, B. A. Song and S. Yang, *Sens. Actuator B*, 2017, **241**, 168-173.
2. M. Saleem and K. H. Lee, *J. Lumin.*, 2014, **145**, 843-848.
3. a) L. Guo, Y. Xu, A. R. Ferhan, G. Chen and D. H. Kim, *J. Am. Chem. Soc.*, 2013, **135**, 12338-12345; b) X. Yang, Y. Luo, Y. Zhuo, Y. Feng and S. Zhu, *Anal. Chim. Acta.*, 2014, **840**, 87-92.
4. G. P. McMahon and M. T. Kelly, *Anal. Chem.*, 1998, **70**, 409-414.

5. R. Pirker, C. W. Huck, M. Popp and G. K. Bonn, *J. Chromatogr. B*, 2004, **809**, 257-264.
6. a) J. Klimeš, J. Sochor, M. Zahradníček and J. Sedláček, *J. Chromatogr.*, 1992, **584**, 221-228; b) J.-H. Liu and P. C. Smith, *J. Chromatogr.*, 1996, **675**, 61-70.
7. R. Bosco, E. Daeseleire, E. Van Pamel, V. Scariot and L. Leus, *J. Agric. Food Chem.*, 2014, **62**, 6278-6284.
8. P. Chocholouš, P. Holík, D. Šatínský and P. Solich, *Talanta*, 2007, **72**, 854-858.
9. S. S. Hassan and M. A. Hamada, *Analyst*, 1988, **113**, 1709-1713.
10. Y. S. Fung and S. F. Luk, *Analyst*, 1989, **114**, 943-945.
11. M. R. Gomez, R. A. Olsina, L. D. Martínez and M. F. Silva, *Talanta*, 2003, **61**, 233-238.
12. P. Bouvrette and J. H. T. Luong, *Anal. Chim. Acta.*, 1996, **335**, 169-175.
13. C. Marťın and E. Domínguez, *J. Pharmaceut. Biomed.*, 1999, **19**, 107-113.
14. M. M. Karim, H. S. Lee, Y. S. Kim, H. S. Bae and S. H. Lee, *Anal. Chim. Acta.*, 2006, **576**, 136-139.
15. O. Bunkoed and P. Kanatharana, *Luminescence*, 2015, **30**, 1083-1089.